AD-A043 296 RCA LABS PRINCETON N J F/G 17/5
GRANULAR MATERIALS FOR UV FILTER.(U)
MAY 77 E K SICHEL, J I GITTLEMAN N00014-76-C-0858
UNCLASSIFIED PRRL-77-CR-19 NL

| OF |
AD
A043296

END
DATE
FILMED
9-77
DDC

UNCLASSIFIED

SECURITY CLASSIFICATION OF THIS PAGE (When Data Entered)

| REPORT DOCUMENTATION PAGE | READ INSTRUCTIONS BEFORE COMPLETING FORM |
|---|---|
| 1. REPORT NUMBER: Final rept. 1 May 76 - 30 Apr 77 (9) | 2. GOVT ACCESSION NO. / 3. RECIPIENT'S CATALOG NUMBER |
| 4. TITLE (and Subtitle): GRANULAR MATERIALS FOR UV FILTER. (6) | 5. TYPE OF REPORT & PERIOD COVERED: Final Report (5-1-76 to 4-30-77) |
| | 6. PERFORMING ORG. REPORT NUMBER: PRRL-77-CR-19 (14) |
| 7. AUTHOR(s): E. K. Sichel and J. I. Gittleman (10) | 8. CONTRACT OR GRANT NUMBER(s): N00014-76-C-0858 (15) new |
| 9. PERFORMING ORGANIZATION NAME AND ADDRESS: RCA Laboratories, Princeton, New Jersey 08540 | 10. PROGRAM ELEMENT, PROJECT, TASK AREA & WORK UNIT NUMBERS |
| 11. CONTROLLING OFFICE NAME AND ADDRESS: Office of Naval Research, Department of the Navy, Arlington, Virginia 22217 (11) | 12. REPORT DATE: May 1977 / 13. NUMBER OF PAGES: 31 |
| 14. MONITORING AGENCY NAME & ADDRESS (if different from Controlling Office) (12) 39p. | 15. SECURITY CLASS. (of this report): Unclassified / 15a. DECLASSIFICATION/DOWNGRADING SCHEDULE: N/A |

16. DISTRIBUTION STATEMENT (of this Report)

Approved for public release; distribution unlimited.

17. DISTRIBUTION STATEMENT (of the abstract entered in Block 20, if different from Report)

18. SUPPLEMENTARY NOTES

19. KEY WORDS (Continue on reverse side if necessary and identify by block number)

Granular metal
Cermet
Optical filter
Maxwell-Garnett theory
Magnesium
Magnesium fluoride

20. ABSTRACT (Continue on reverse side if necessary and identify by block number)

We have tested the potential of several sputtered cermets as a component in a solar-blind UV filter. Films made of metal grains embedded in an insulating matrix may exhibit a strong optical absorption which is absent in the bulk metal. The dimensions of the grains are much smaller than the wavelengths of the radiation which is relevant to the filter problem. Under this condition, the optical

DD FORM 1 JAN 73 1473

UNCLASSIFIED

SECURITY CLASSIFICATION OF THIS PAGE (When Data Entered)

299 000

/B

20.

properties of the cermet may be described by the Maxwell-Garnett theory. We co-sputtered Mg with MgO and $MgF_2$ and Al with $Al_2O_3$ and $SiO_2$. The optical absorption desired was found in cermets of Mg-$MgF_2$ when the $MgF_2$ sputtering target was a single crystal. The observed optical absorption band was broad and weak, due to small metal grain size. Grain growth is required before this material would be suitable for an optical filter. However, it was not possible to promote grain growth by annealing because of reaction with oxygen trapped in the $MgF_2$ matrix which was porous. It is apparent that nonporous $MgF_2$ films must be obtained or another nonreactive matrix material must be found before a satisfactory filter can possibly be fabricated from cermet films. Thus we have not proved the cermet filter to be unattainable. Rather we have discovered the very difficult materials problems which must be overcome to obtain good filter characteristics.

## PREFACE

This Final Report describes research performed during the period 1 May 1976 through 30 April 1977, under Contract N00014-76-C-0858, at RCA Laboratories in the Materials Research Laboratory, Dr. James J. Tietjen, Director. The Project Supervisor was J. I. Gittleman and the Project Scientist was E. Sichel.

The Government Project Monitor is Dr. Van O. Nicolai.

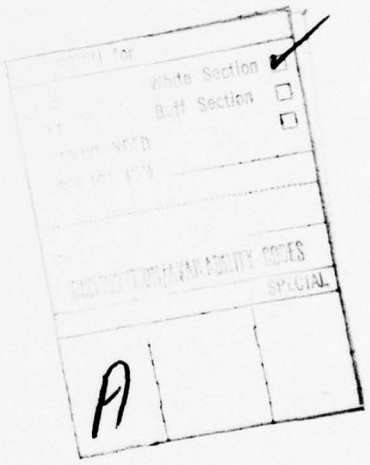

TABLE OF CONTENTS

## LIST OF ILLUSTRATIONS

## SECTION I

## INTRODUCTION

The purpose of this research program was to test the potential of sputtered cermets as a component in a solar-blind UV filter. In particular, the cermet film should be opaque to wavelengths longer than 3000 Å, and transparent at shorter wavelengths. In this report we outline: (1) the theoretical basis of the expectation that an appropriate cermet would have the optical properties required for the filter, (2) the properties which the constituents of the cermet must have for optimum filter performance, and (3) the results of our experimental studies to determine the feasibility of making a cermet filter with the required properties.

The cermet films are formed by co-sputtering a metal and an insulator onto an appropriate substrate. If the constituents are immiscible and the volume fraction of the metal is sufficiently small, the resulting film contains an array of minute metal grains dispersed in an insulating matrix. In general, the size of the metal grains varies from several hundred angstrom units in diameter down to clusters of a few atoms. Thus, the metal grains are much smaller than the wavelengths of the radiation which are relevant to the filter problem.

Composite materials of this type exhibit optical properties quite different from those of the individual components. In addition to the sputtered cermets [1,2], metal dispersions such as colloids [3] and discontinuous metal films [4] have been shown to exhibit a strong optical absorption which is absent in the bulk metal. An example of this is Au colloidal particles suspended in glass in which the absorption peak gives rise to a characteristic ruby-red color.

---

1. R. W. Cohen, G. D. Cody, M. D. Coutts and B. Abeles, Phys. Rev. B8, 3689 (1973).
2. E. B. Priestley, B. Abeles and R. W. Cohen, Phys. Rev. B12, 2121 (1975).
3. R. H. Doremus, J. Chem. Phys. 42, 414 (1965); 40, 2389 (1964).
4. R. W. Tokarsky and J. P. Marton, J. Appl. Phys. 45, 3051 (1974).

The required sharpness of the cutoff of a filter using this characteristic absorption band demands that the scattering time for the conduction electrons in the metal grains be about the same as that in the bulk metal. Since the boundaries of the grains dominate the electron scattering processes in the cermets, the diameter of the metal grains must be of the order of a few hundred angstrom units, as discussed in Section III. We did not expect to find such large metal grains in as-prepared films. However, considerable grain growth can sometimes be induced by annealing [5,6].

5. H. L. Pinch, J. Vac. Sci. Technol. 12, 60 (1975).
6. N. C. Miller, B. Hardiman, and G. A. Shirn, J. Appl. Phys. 41, 1850 (1970).

## SECTION II

## THEORY

There seems to be little doubt that the Maxwell-Garnett equation [7]

$$\frac{\varepsilon - \varepsilon_I}{\varepsilon + 2\varepsilon_I} = x \frac{\varepsilon_m - \varepsilon_I}{\varepsilon_m + 2\varepsilon_I} \tag{1}$$

relating the complex dielectric constant, $\varepsilon$, of the composite to those of the constituents ($\varepsilon_m$ for the metal, and $\varepsilon_I$ for the insulator) gives the best prediction of the optical constants of the sputtered cermets [8]. In Eq. (1), x is the volume fraction occupied by the metal. Furthermore, the metal grains are assumed to be spherical, small, compared with the wavelength and dispersed in the insulating matrix. The dielectric constant $\varepsilon = (\varepsilon_1 + i\varepsilon_2)$ is related to the index of refraction, n, and extinction coefficient, k, as follows:

$$\varepsilon_1 = n^2 - k^2 \text{ and } \varepsilon_2 = 2nk.$$

The dielectric constant of a typical metal is complex and has two contributions.

Thus,

$$\varepsilon_m = \varepsilon_{IB} + \varepsilon_{FE} = \varepsilon_{m1} + i\varepsilon_{m2} \tag{2}$$

where $\varepsilon_{FE}$ is the contribution due to the free (conduction) electrons and $\varepsilon_{IB}$ is the contribution due to bound electrons which can absorb photons by making an interband transition. As we shall see, it is essential for the free electron contribution to dominate $\varepsilon_m$ in order to obtain a filter with sharp cutoff characteristics. In the case of the free electrons, there is a frequency, the plasma frequency, $\omega_p$, at which the real part of $\varepsilon_{FE} = 0$. For most metals the plasma wavelength $\lambda_p$ ( $= \frac{2\pi c}{\omega_p}$, c = speed of light) is about 1000 Å. At longer wavelengths $\mathrm{Re}(\varepsilon_{FE})$ is negative and diverges at infinite

7. J. C. Maxwell-Garnett, Philos. Trans. R. Soc. Lond. 203, 385 (1904); 205, 237 (1906).
8. J. I. Gittleman and B. Abeles, Phys. Rev. B15, 3273 (1977).

wavelength. At shorter wavelengths it is positive, approaching unity as $\lambda << \lambda_p$. In general $\varepsilon_{FE}$ is given by [9]

$$\varepsilon_{FE} = 1 + i \frac{\omega_p^2 \tau}{\omega(1 - i\omega\tau)} , \tag{3a}$$

$$\mathrm{Re}(\varepsilon_{FE}) = \left(1 - \frac{\omega_p^2 \tau^2}{1 + \omega^2\tau^2}\right) , \tag{3b}$$

$$\mathrm{Im}\ (\varepsilon_{FE}) = \frac{\omega_p^2 \tau}{\omega(1 + \omega^2\tau^2)} , \tag{3c}$$

where $\tau$ is the scattering time of the conduction electrons and $\omega = 2\pi c/\lambda$.

When a granular metal is formed, as in a cermet, then it can readily be seen from Eq. (1) that the composite not only exhibits a plasma resonance similar to an ordinary metal, but also exhibits an anomalous absorption. If we can ignore the imaginary part of the dielectric constants it can be seen that $\varepsilon = 0$ (plasma resonance) when the left-hand side of Eq. (1) becomes - 1/2. This will occur at a frequency $\omega_p'$ for which

$$\varepsilon_m(\omega_p') = - \frac{2(1 - x)}{1 + 2x} \varepsilon_I . \tag{4}$$

Thus, for a plasma resonance to occur in the composite, $\varepsilon_m(\omega_p')$ *must be negative*. At the anomalous absorption, $\omega = \omega_a$ and the left-hand side of Eq. (1) approaches unity since $\varepsilon(\omega_a) >> \varepsilon_I$. This occurs if

$$\varepsilon_m(\omega_a) = - \frac{2 + x}{1 - x} \varepsilon_I \tag{5}$$

and again $\varepsilon_m(\omega_a)$ *must be negative*. If $\varepsilon_{IB}$ is neglected and the electron scattering time $\tau$ is large so that $\omega_p\tau$, $\omega_p'\tau$, and $\omega_a\tau$ are all large compared with unity, $\varepsilon_m(\omega) = 1 - (\frac{\lambda}{\lambda_p})^2$ from Eqs. (3), (4) and (5) give

$$\lambda_p'^2 = \lambda_p^2 \left[1 + \frac{2(1 - x)}{1 + 2x} \varepsilon_I\right] \tag{6a}$$

and

$$\lambda_a^2 = \lambda_p^2 \left[1 + \left(\frac{2 + x}{1 - x}\right) \varepsilon_I\right] \tag{6b}$$

---

9. J. M. Ziman, *Principles of the Theory of Solids*, (Cambridge University Press, 1965) Chapter 8.

The real part of $\varepsilon_{IB}$ is generally positive. Therefore, if it is too large to be neglected, the magnitude of $\varepsilon_{FE}$ must be larger than $\varepsilon_{IB}$ for the composite to exhibit a plasma resonance and an absorption anomaly. In this case we obtain from Eq. (4)

$$(\lambda_p')^2 = (\lambda_p)^2 \left[1 + \frac{2(1 - x)}{1 + 2x} \varepsilon_I + \varepsilon_{IB} (\omega_p') \right] \tag{7}$$

and a similar expression from Eq. (5).

Qualitatively, the optical properties of a cermet film exhibiting a plasma resonance and an absorption anomaly can be described as follows: For $\lambda < \lambda_p'$ or $\lambda > \lambda_a$ the film is transmitting, its behavior similar to a transparent dielectric; for $\lambda_p' < \lambda < \lambda_a$ the film is highly reflecting and absorbing with little transmittance, behavior similar to that of a metal. In Fig. 1 is shown the real and imaginary parts of $\varepsilon$ as a function of wavelength, computed from Eq. (1). Here $\varepsilon_m = \varepsilon_{FE}$, $\varepsilon_I = 3.7$ and $\lambda_p = 1200$ Å and $\tau = 1.0 \times 10^{-14}$ s. It should be noted the wavelength dependence of $\varepsilon$ is similar to that of an ionic crystal near its *restrahlen band*. This behavior, of course, is the basic property needed for the filter.

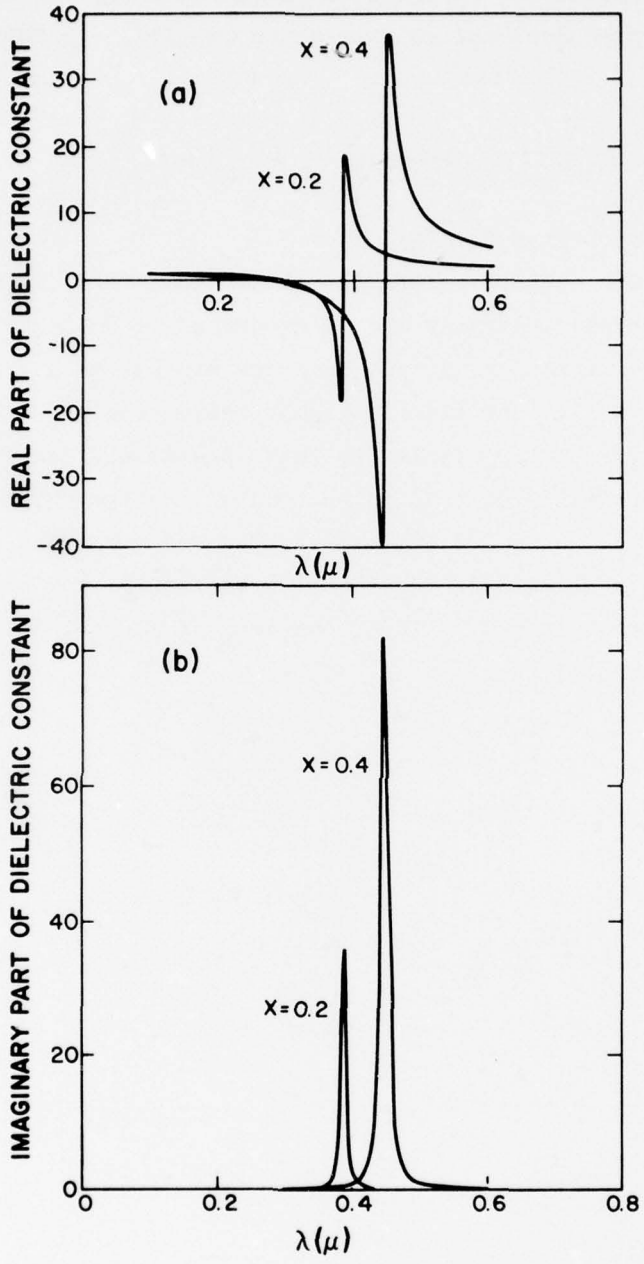


Figure 1. (a) The real part, and (b) the imaginary part of the dielectric constant of a free electron metal calculated from Eqs. (1) and (3) for two values of the metal volume fraction, x. The plasma wavelength ($\lambda_p$) is 1200 Å, $\tau = 1.0 \times 10^{-14}$ s and $\varepsilon_I = 3.7$.

## III. MATERIAL REQUIREMENTS

This section is concerned with the properties of the constituents of the cermet which are needed to obtain good filter characteristics. In the case of the insulating matrix there are two requirements. The insulator must be transparent in the wavelength range of interest and its dielectric constant must be sufficiently large to permit "tuning" of the filter by adjusting the composition (see Eq. (6)). For the purposes of demonstrating feasibility, the requirement of transparency is the only important one. Finding the optimum insulator which maximizes tunability was considered an unnecessary complication at this stage.

The severest requirements rest with the metal component. First, its optical properties must not be dominated by interband transitions. The transition metals are not suitable for this reason. In the noble metals such as Au and Ag, $\varepsilon_{IB}$ is not so large as to preclude the desired properties, but it is large enough (See Eq. (7)) to place the resonance at wavelengths too long to be useful [1]. Promising candidates can be found among the alkali metals, alkaline earth metals, and aluminum. The most favorable of these are Al and Mg, whose optical properties are dominated by free electrons, and these metals are relatively easy to handle. Magnesium, ($\lambda_p \simeq 1200$ Å) is a somewhat better prospect than aluminum ($\lambda_p \simeq 900$ Å).

Another requirement is that the metal grains be sufficiently large. In a bulk pure metal at room temperature the conduction electrons have a mean free path of about 200 Å corresponding to a scattering time $\tau$ of about $1 \times 10^{-14}$ s. Scattering is due to collisions with phonons. In cermets, where the mean grain size may be 20 Å or less and electron scattering is dominated by collisions with the boundary, $\tau$ will be correspondingly less. Excessively small values of $\tau$ will have a drastic effect on the quality of the filter. In general, the smaller the value of $\tau$, the weaker and broader will be the anomaly shown in Fig. 1. The broadening reduces the sharpness of the filter cutoff and the weakening will enhance the effect of interband transitions. Figure 2 shows the optical density of three hypothetical cermet films. The metal component of each is a free electron metal. The films differ only in the values of $\tau$. Here the rounding due to excessive scattering becomes clear. Therefore,

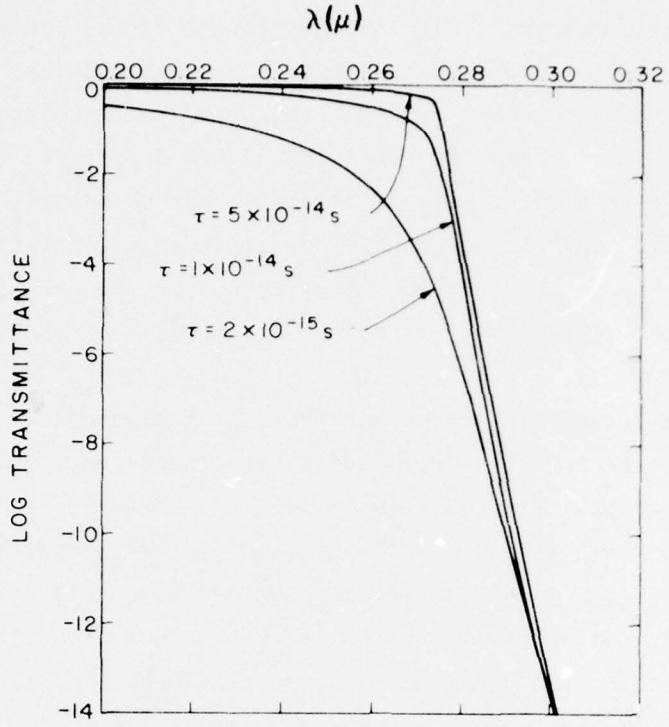


Figure 2. Log of transmittance vs wavelength calculated for three cermets, each 0.75 μm thick and composed of 20 vol % free electron metal ($\lambda_p$ = 1270 Å) dispersed in $Al_2O_3$. The mean electron scattering time of each is indicated in the figure.

it is absolutely essential that the metal grain size be controllable, presumably through heat treatment.

The following section outlines our experimental efforts. Both Al and Mg cermets have been studied and the degree to which they meet the above requirements will be discussed.

## SECTION IV

## RESULTS

Magnesium and aluminum were the metals of choice in this program because their optical properties are dominated by the conduction electrons.

### A. MAGNESIUM CERMETS

We prepared thin films of Mg by evaporation and sputtering and by reactive sputtering in the presence of oxygen to test the stability of the films in the atmosphere.

The plasma frequency of Mg($\lambda_p \simeq 0.117$ μ) can be computed from optical data [10]. The free electron contribution to the optical constants of Mg was generated for different values of $\tau$ using Eq. (3). The films should become more transparent in the ultraviolet than they are in the visible. This is characteristic of a (free electron) metal [9], of which magnesium is a good example [10]. Note that if the electron scattering time becomes too short, e.g. $\sim 10^{-16}$ s, the material would not behave like a metal. Figure 3 shows the computed optical density of a 500-Å film of pure Mg with scattering times $\tau = 10^{-15}$ s, $3 \times 10^{-16}$ s, and $10^{-16}$ s.

Figure 4 shows the observed optical density of a thin film of Mg reactively sputtered with a small amount of oxygen. All optical measurements were done with a Cary 14 spectrophotometer and, below 1900 Å, with a Jarrell-Ash VUV spectrometer. The character of the results for $\lambda \gtrsim 0.3$ μm indicate that metallic Mg was sputtered successfully. However, within a few days at room atmosphere, the Mg films had oxidized. Attempts to seal the surface with a layer of $SiO_2$ were unsuccessful, probably because the Mg films are porous. The solid curve in Fig. 5 is the optical density computed using the optical constants for pure Mg [10] ($\tau \sim 10^{-14}$ s). As can be seen, the agreement with theory is very good for $\lambda \gtrsim 0.3$ μm.

Although the general feature of Fig. 5 indicates metallic Mg, there is an excess absorption in the UV which is due to the presence of MgO. Sometimes,

---

10. H. J. Hagemann, W. Audat, and C. Kunz, Deutsches Elektronen-Synchrotron, 2 Hamburg 52, May 1974.
11. B. Abeles, "Granular Metal Films," Applied Solid State Science 6, 1976, Academic Press.

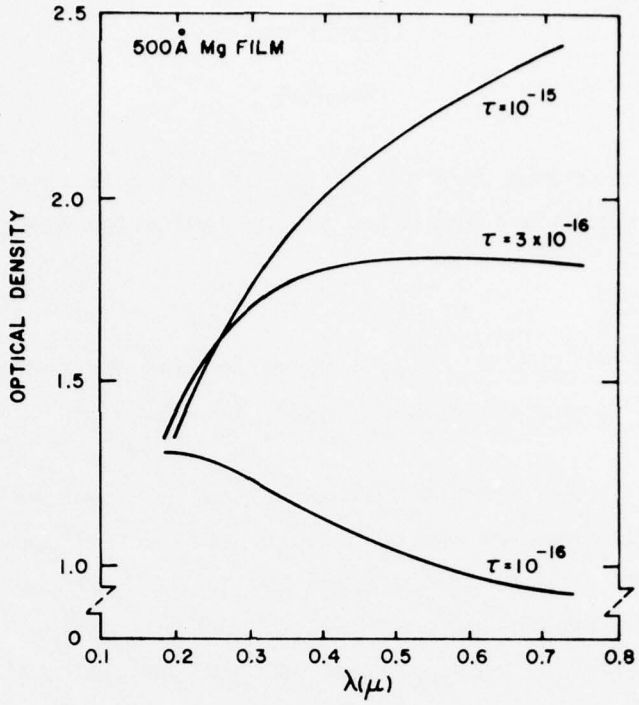


Figure 3. Optical density of thin films of Mg metal computed for various electron scattering times.

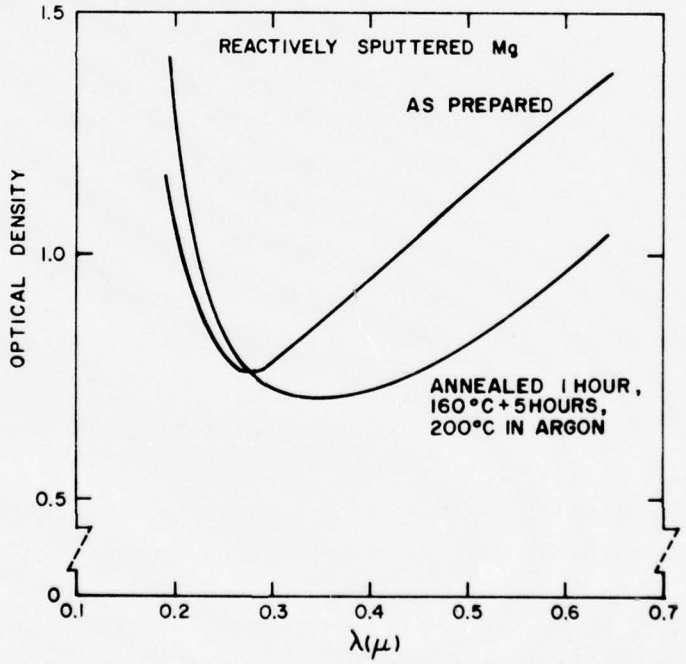


Figure 4. Optical density of thin films of reactively sputtered Mg, as prepared and annealed.

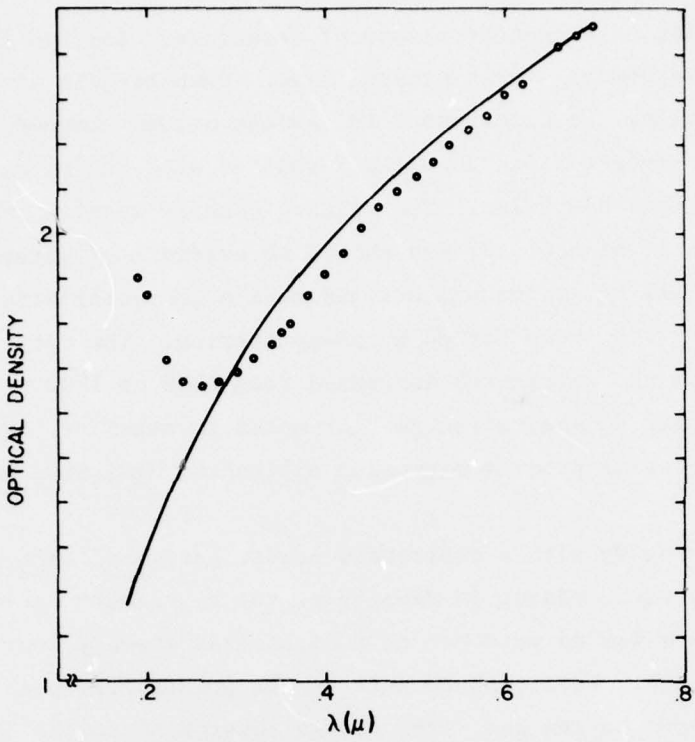


Figure 5. Optical density vs wavelength. Solid curve: computed for 500 Å. Mg film using published values of optical constants[1] ($\tau \sim 10^{-14}$ s). Points: Experimental data for 500-Å film of Mg sputtered in Ar containing $10^{-6}$ torr $O_2$.

annealing samples promotes grain growth in cermets or coalescence of metallic patches [11] in discontinuous films which increases the electron mean free path and increases $\tau$. Annealing the thin films of Mg had the opposite effect: there was loss of Mg metal and an increase in the UV absorption as seen in Fig. 4. Since all annealing was done either in an inert atmosphere of argon or in a reducing atmosphere of hydrogen, we conclude that the films contained trapped atmospheric oxygen.

Composite materials with magnesium metal were prepared by sputtering. These included Mg-MgO, Mg-$SiO_2$, and Mg-$MgF_2$. We discuss each in turn.

Films of Mg, co-sputtered with MgO gave films whose optical density increased monotonically with energy from the visible to the ultraviolet. Annealing did not change the general features of the optical density spectrum. Annealing temperatures were generally about 200°C. Higher temperature did not improve the results. The rising absorption in the UV is probably due to the formation

of MgO containing high concentrations of vacancies. The MgO sputtering target was a compressed powder, a hot pressed disc. Such targets are porous and trap atmospheric oxygen. We expect that the excess oxygen trapped in the MgO target, (plus any $MgO_2$ present as an impurity,) reacted with the Mg metal, leaving no metallic Mg in the thin films. The optical density spectra of the Mg-MgO films was characteristic of MgO [12] and showed no evidence of either metallic behavior or of small Mg grains which would have a characteristic absorption peak.

Films of Mg-$SiO_2$ were formed by co-sputtering. The optical density rose monotonically as the wavelength decreased from 7000 to 1900 Å. There was no evidence of either an absorption peak or metallic behavior. We assume that during the sputtering process magnesium silicates, MgO, SiO, and Mg-Si compounds were formed.

Co-sputtering Mg with a compressed powder target of $MgF_2$ gave the familiar optical density curve rising in density as the wavelength decreased from 7000 to 2000 Å. There was no evidence of a dielectric anomaly, nor did annealing produce any change. We attribute this to the porous $MgF_2$ compressed powder target which traps oxygen gas. The excess absorption in the UV is probably due to the formation of MgO. On the other hand, when we co-sputtered Mg with single crystal $MgF_2$ the absorption peak predicted by theory was obtained. $MgF_2$ was selected as the insulating matrix because it is an insulator without oxygen and is not expected to react with Mg. Further, the single crystal $MgF_2$ target does not trap atmospheric oxygen as the compressed powder target does.

The predicted optical density spectra of Mg-$MgF_2$ is shown in Figs. 6 (a), 6 (b) and 6 (c) for different compositions and electron scattering times. The optical constants of $MgF_2$ were assumed to be $n = 1.4$, and $k = 0$. Our experimental results for films of Mg-$MgF_2$ are shown in Fig. 7. There is a dielectric anomaly near 2500 Å. Figure 8 shows the theoretical curves for different $\tau$'s and the experimental spectrum for a 36 vol % Mg sample, all superimposed on the same graph. It can be seen that scattering time $\tau$ of about $2 \times 10^{-16}$ s would result in good agreement between observation and the calculated optical density. If we assume the Fermi velocity $v_F \sim 2 \times 10^8$ cm/s, then $\ell \sim 4 \times 10^{-8}$ cm. This corresponds to a Mg grain consisting of a cluster of a few atoms.

---

12. A. J. Moses, ed., *Handbook of Electronic Materials*, Vol. 1, Optical Materials Properties, (Plenum Press, New York, 1971).

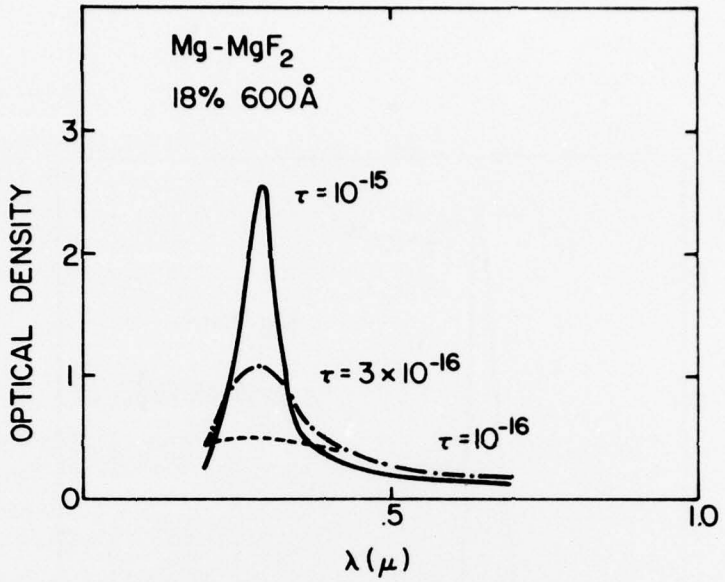


Figure 6(a). Theoretical optical density spectra of Mg-$MgF_2$ cermets for 18 vol % Mg metal embedded in $MgF_2$ matrix.

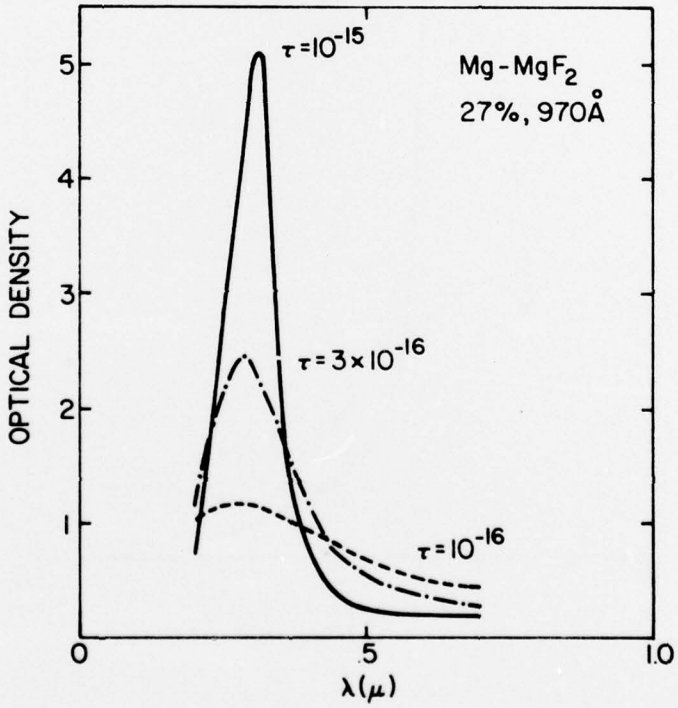


Figure 6(b). Theoretical optical density spectra of Mg-$MgF_2$ cermets for 27 vol % Mg metal embedded in $MgF_2$ matrix.

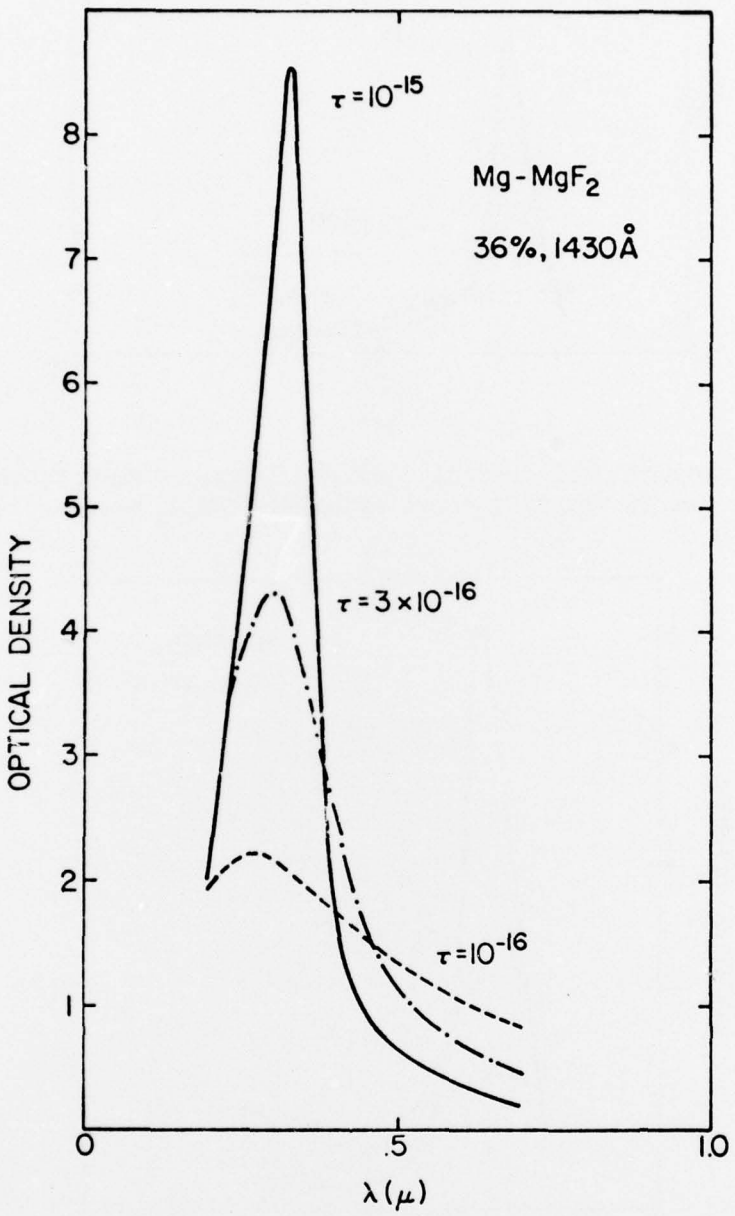


Figure 6(c). Theoretical optical density spectra of Mg-$MgF_2$ cermets for 36 vol % Mg metal embedded in $MgF_2$ matrix.

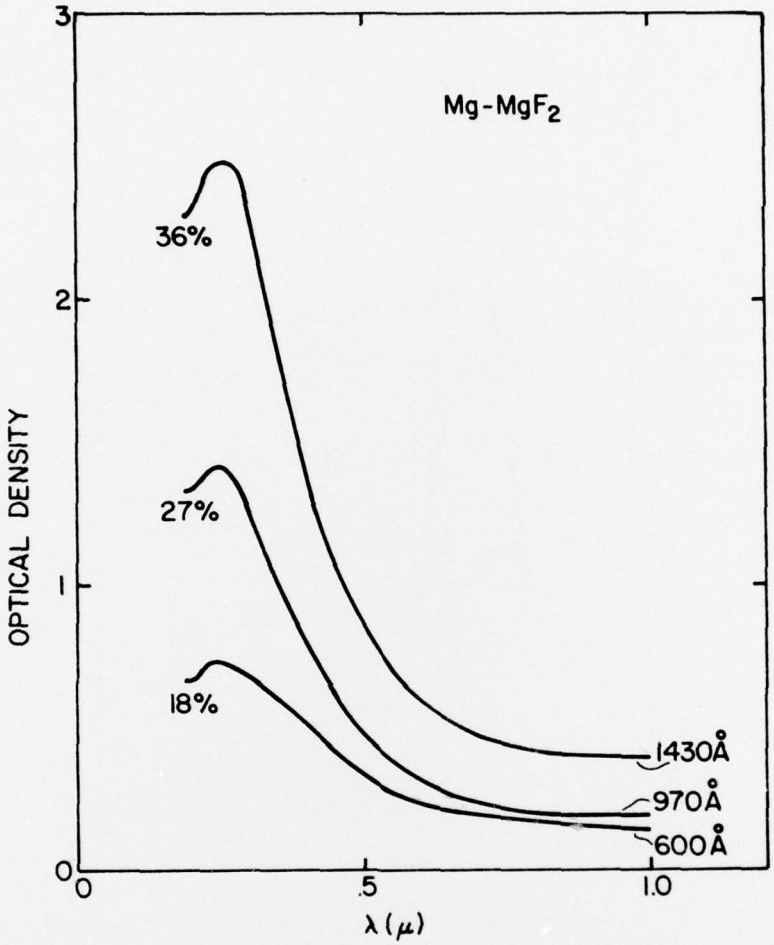


Figure 7. Experimental optical density spectra of $Mg-MgF_2$ cermets.

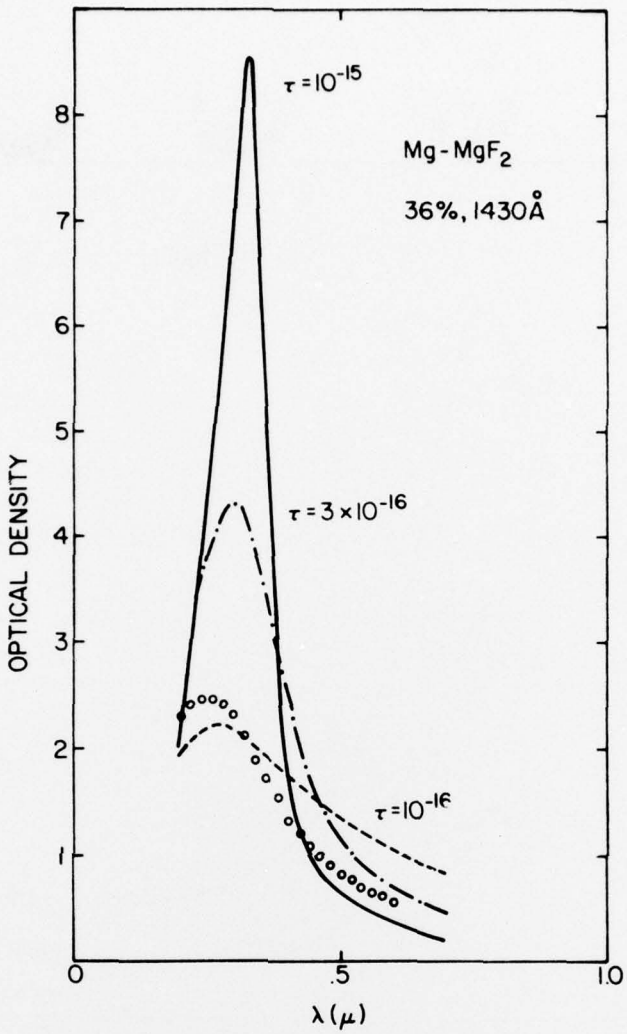


Figure 8. Theoretical optical density spectra of $Mg-MgF_2$ cermet for 36 vol % Mg metal embedded in $MgF_2$ matrix with experimental data (circles) superimposed.

Electron micrographs of the $Mg-MgF_2$ samples showed a variety of Mg grain sizes from 150 Å down to the resolution of the microscope, about 20 Å for magnesium. However, we believe that a larger number of magnesium grains exist in clusters of a few atoms. Figures 9 and 10 are dark-field micrographs of a 82 vol % Mg sample and a 43 vol % Mg sample. In Fig. 9, Mg metal was the only crystalline material that was found in the diffraction pattern. The visible (white) grains of Mg do *not* take up most of the volume, indicating that the


**Figure 9.** Transmission electron micrograph of $Mg-MgF_2$ cermet, nominally 82 vol % Mg.

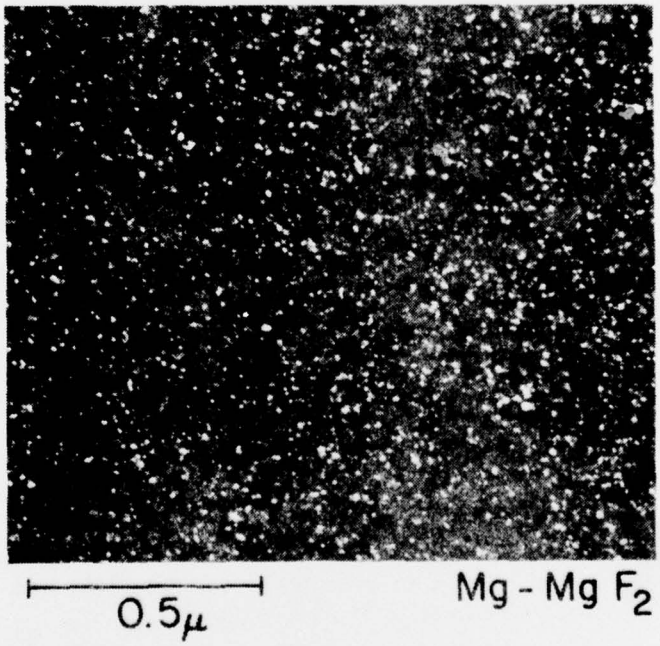


**Figure 10.** Transmission electron micrograph of $Mg-MgF_2$ cermet, nominally 43 vol % Mg.

rest of the Mg grains are oriented to diffract the electron beam out of the field of view. In Fig. 10 the visible grains are predominantly Mg metal, although a small fraction are MgO and $MgO_2$.

Auger electron analysis shows that the Mg-$MgF_2$ samples consist of a surface layer containing MgO and no metal. Below the oxidized layer, grains of metallic Mg are found, in addition to MgO, which give rise to the optical dielectric anomaly. The depth of the surface layer increases with the age of the specimen. These results suggest that the sputtered $MgF_2$ matrix is quite porous to atmospheric oxygen.

In Fig. 11 are shown the optical density spectra of 34 vol % Mg (nominal) and 77 vol % Mg (nominal) samples. The upper curve shows the characteristic metallic behavior, even including a broad interband absorption in the IR. Note that there is still some excess absorption in the UV, even in the metallic sample.

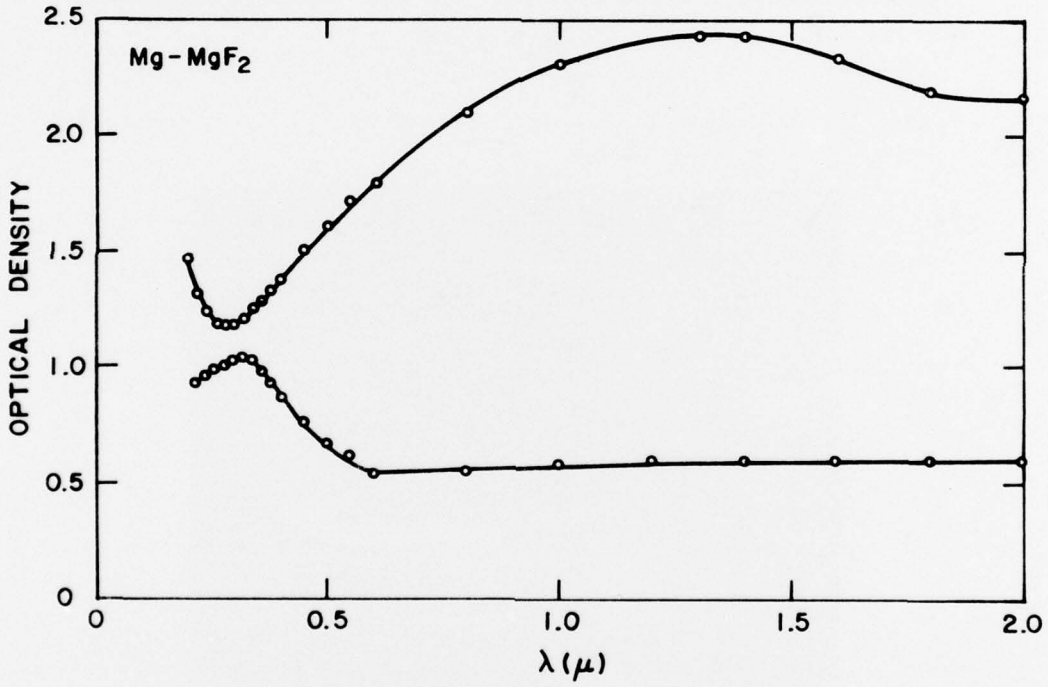


Figure 11. Experimental optical density spectra of Mg-$MgF_2$ cermets. The upper curve is nominally 77 vol % Mg and the lower curve is nominally 34 vol % Mg.

Examination of Mg-$MgF_2$ samples of Mg $F_2$ substrates in the VUV to 1250 Å showed that the optical density of the $MgF_2$-rich samples in Fig.7 does not drop to low values on the high energy side of the absorption peak. We attribute this to color centers in the $MgF_2$, or to the formation of MgO. It has been shown that the packing density of $MgF_2$ may be as low as 74% [13] unless the films are deposited on heated substrates. A porous material will be easily attacked by oxygen. Annealing did not promote grain growth but resulted in the apparent loss of Mg as shown in Fig. 12. From the results of the Auger spectroscopy, we conclude that the loss results from reaction with absorbed oxygen.

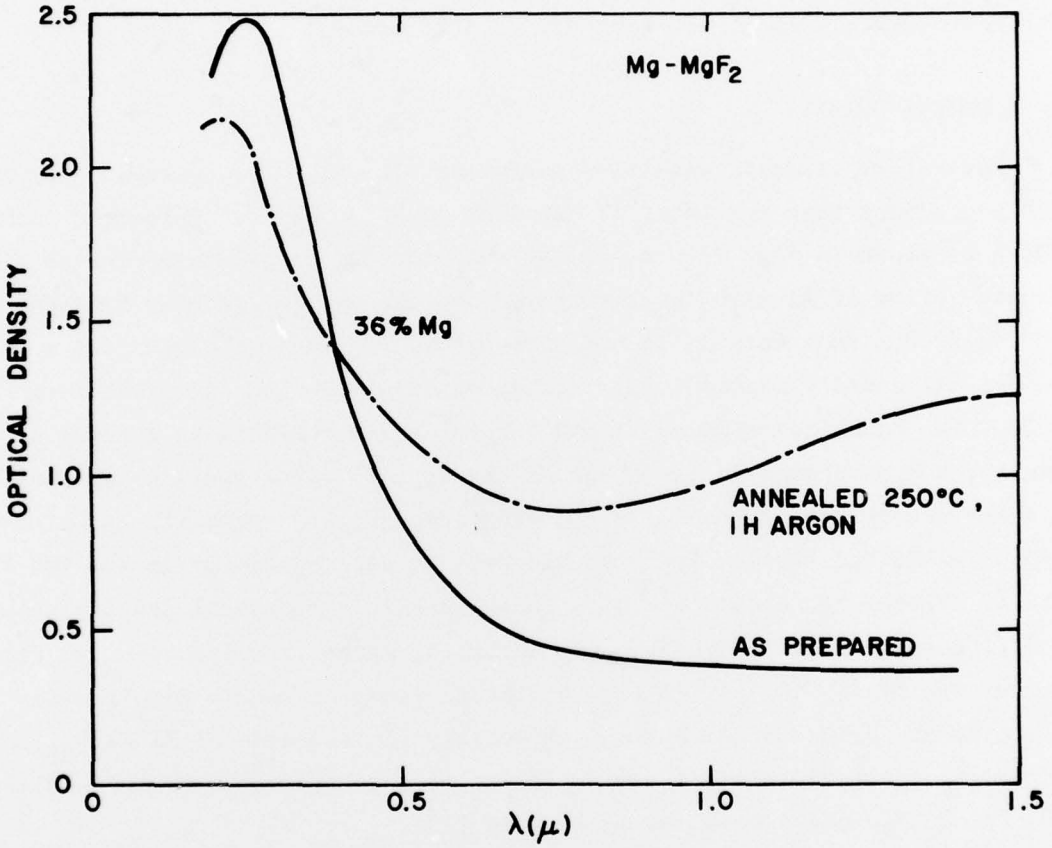


Figure 12. Experimental optical density spectra of Mg-$MgF_2$ cermets, 36 vol % Mg, as prepared and annealed.

We were unable to determine the composition of the Mg-$MgF_2$ samples by wet chemical analysis. To determine the amount of Mg that exists as metallic Mg, a determination of the weight of F in the sample was made and then it was assumed that all F was bound in $MgF_2$ molecules. The results were irreproducible. We therefore used a computer-generated composition profile [14] using the sputtering target geometry and the measured thickness gradient of a deposited Mg-$MgF_2$ sample. These are the volume compositions cited in the figures and should be treated as nominal values. Whenever MgO or $MgO_2$ is formed at the expense of Mg, the composition of the sample is changed. Both the electron micrographs and the Auger analysis found MgO present in the samples. Of course the computer-generated compositions profiles do not take oxides into account.

## B. ALUMINUM CERMETS

Several experiments were also performed with Al metal systems. The M-G theory predicts that grains of Al embedded in $Al_2O_3$ have a dielectric anomaly near 2500 Å as shown in Fig. 13. A similar result would be predicted for an Al-$SiO_2$ cermet. Films of Al-$Al_2O_3$ were prepared and the optical density measured from 2000 to 7000 Å on a Cary 14 spectrophotometer. Instead of exhibiting a maximum, the optical density monotonically increased as wavelength decreased from 7000 to 2000 Å. Annealing samples at 600°C for 1 1/2 h resulted in a lower optical density, but no change in the shape of the curve. All annealing was done in an inert atmosphere (argon) or a reducing atmosphere (hydrogen). Samples of Al-$SiO_2$ exhibited similar behavior and were studied optically in the VUV to 1650 Å. There was no evidence of a sharp peak in the optical density below 2000 Å, but the optical density does saturate, rather than continue to rise. In the case of Al-$SiO_2$, it is likely that Al tends to reduce $SiO_2$ forming silicates and oxides of Al during sputtering. In the case of Al-$Al_2O_3$, the formation of suboxides of Al could reduce the amount of free Al. There are reports of $Al_2O$ and AlO in the literature [15].

---

13. E. Ritter in G. Hass, ed., *Physics of Thin Films*, Vol. 8 (Academic Press, New York, 1975).
14. J. J. Hanak, H. W. Lehman, and R. K. Wehner, J. Appl. Phys. 43, 1666 (1972).
15. Rodney P. Elliott, ed., *Constitution of Binary Alloys*, (McGraw Hill, N.Y., 1965) First Supplement.

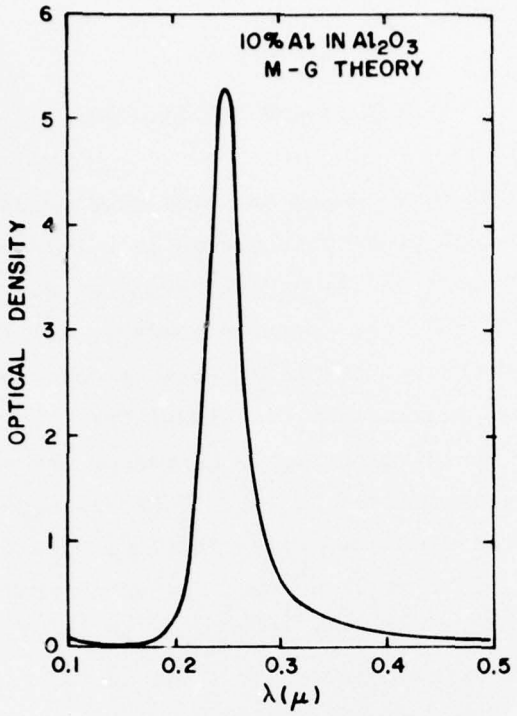


Figure 13. Theoretical optical density spectrum of Al-$Al_2O_3$ cermet for 10 vol % Al metal embedded in $Al_2O_3$ matrix.

C. OTHER SYSTEMS

Finally, it should be mentioned that Na metal in thin or discontinuous films would have the desired optical properties for a UV filter [16]. In fact, a number of the alkali metals are likely to have desirable optical properties. However, they are even more reactive than Al and Mg and are difficult to handle as they are not stable in room atmosphere.

16. Charles Kittel, *Introduction to Solid State Physics*, (John Wiley & Sons, N. Y., 1976) 3rd ed., p. 229.

## SECTION V

## SUMMARY AND CONCLUSIONS

Cermets of Al and Mg were chosen as those composites which would most closely exhibit the optical properties needed in a solar-blind filter. Films produced by co-sputtering Al and $Al_2O_3$ (alumina), Al and $SiO_2$, Mg and MgO (pressed powder), and Mg and $MgF_2$ (pressed powder), all failed to exhibit the optical absorption band characteristic of cermets containing grains of a free electron metal dispersed in a transparent insulator. In the case of Al-$SiO_2$ there is evidence that the aluminum tends to reduce the quartz. Thus, this system is not a completely immiscible one. There is also evidence in the literature indicating that the aluminum-oxygen contains suboxides of Al. Thus, co-sputtering Al with either $Al_2O_3$ or $SiO_2$ failed to produce Al grains dispersed in an insulator. In the case of Mg-MgO, it is clear the pressed powder target contained excess oxygen, either as absorbed $O_2$ or as $MgO_2$ or both, which oxidized the Mg metal. The pressed powder $MgF_2$ target clearly contained absorbed $O_2$.

On the other hand, the desired cermet (Mg-$MgF_2$) was formed when a single crystal $MgF_2$ target was used. However, the $MgF_2$ matrix was found to be porous and contained a large quantity of atmospheric oxygen. The presence of the $O_2$ limited the shelf life of the cermets and, more seriously, prevented the execution of definitive annealing studies.

Thus, before Mg-$MgF_2$ cermets can be made with the desired optical properties, methods of deposition must be found in which the $MgF_2$ matrix is nonporous, or in which the cermet is sealed before exposure to the atmosphere.

Other alkaline earth metals and some of the alkali metals may be preferable to magnesium. Indeed, there is evidence in the literature that sodium may be suitable. Materials suitable for the solar-blind filter are reactive metals; dispersing large grains of a reactive metal, a few hundred angstroms in diameter, has proved to be a difficult materials problem, one whose surface we have only scratched.

## REFERENCES


1. R. W. Cohen, G. D. Cody, M. D. Coutts and B. Abeles, Phys. Rev. B8, 3689 (1973).
2. E. B. Priestley, B. Abeles and R. W. Cohen, Phys. Rev. B12, 2121 (1975).
3. R. H. Doremus, J. Chem. Phys. 42, 414 (1965); 40, 2389 (1964).
4. R. W. Tokarsky and J. P. Marton, J. Appl. Phys. 45, 3051 (1974).
5. H. L. Pinch, J. Vac. Sci. Technol. 12, 60 (1975).
6. N. C. Miller, B. Hardiman, and G. A. Shirn, J. Appl. Phys. 41, 1850 (1970).
7. J. C. Maxwell-Garnett, Philos. Trans. R. Soc. Lond. 203, 385 (1904); 205, 237 (1906).
8. J. I. Gittleman and B. Abeles, Phys. Rev. B15, 3273 (1977).
9. J. M. Ziman, *Principles of the Theory of Solids*, (Cambridge University Press, 1965) Chapter 8.
10. H. J. Hagemann, W. Audat, and C. Kunz, Deutsches Elektronen-Synchrotron, 2 Hamburg 52, May 1974.
11. B. Abeles, "Granular Metal Films," Applied Solid State Science 6, 1976, Academic Press.
12. A. J. Moses, ed., *Handbook of Electronic Materials*, Vol. 1, Optical Materials Properties, (Plenum Press, New York, 1971).
13. E. Ritter in G. Hass, ed., *Physics of Thin Films*, Vol. 8 (Academic Press, New York, 1975).
14. J. J. Hanak, H. W. Lehman, and R. K. Wehner, J. Appl. Phys. 43, 1666 (1972).
15. Rodney P. Elliott, ed., *Constitution of Binary Alloys*, (McGraw Hill, N.Y., 1965) First Supplement.
16. Charles Kittel, *Introduction to Solid State Physics*, (John Wiley & Sons, N. Y., 1976) 3rd ed., p. 229.

## DISTRIBUTION LIST

Naval Electronics Lab Center
Tech Library
San Diego, CA 92152

Naval Undersea Center
Technical Library
San Diego, CA 92132

Naval Surface Weapons Center
Technical Library
Dahlgren, VA 22448

Naval Ship R&D Center
Central Library (Code L42 & L43)
Bethesda, MD 20084

Naval Surface Weapons Center
Technical Library
Silver Spring, MD 20910

Naval Avionics Facility
Technical Library
Indianapolis, IN 46218

University of California
Lawrence Livermore Lab
Attn: Dr. W.F. Krupke
P.O. Box 808
Livermore, CA 94550

Rennselaer Polytechnic Inst
Materials Eng Div
Attn: Dr. J.B. Hudson
Troy, NY 12191

MIT - Dept of Metallurgy &
Materials Science
Attn: Dr. K.H. Johnson
Cambridge, MA 02139

University of Texas
Dept of Physics
Attn: Dr.W.D. McCormick
Austin, TX 78712

Univ of California at Berkely
Dept of Chemistry
Attn: G.A. Somorjai
Berkely, CA 94720

California Inst of Technology
Div of Chemistry & Chem Eng
Attn: Dr. R.W. Vaughn
Pasadena, CA 91125

INTELCOM RAD TECH
Attn: Dr. D.A. Vroom
P.O. Box 80817
San Diego, CA 92138

Northwestern University
Attn: Dr. J.B. Wagner, Jr
Evanston, IL 60201

University of Texas
Dept of Chemistry
Attn: J.M. White
Austin, TX 78712

Department of Commerce
National Bureau of Standards
Surface Chemistry Section
Attn: Dr. J.T. Yates, Jr
Washington, DC 20234

International Business Machines
T.J. Watson Research Center
Attn: J.E. Demuth
P.O. Box 218
Yorktown Heights, NY 10598

University of Illionis
Dept of Physics
Attn: Dr. C.P. Flynn
Urbana, IL 61801

University of Cal at San Diego
Department of Physics
Attn: Dr. W. Kohn
La Jolla, CA 92037

U.S. Department of Commerce
National Bureau of Standards
Surface Processes & Catalysis
Attn: Dr. T.E. Madey
Washington, DC 20234

University of Maryland
Director, Ctr of Materials Res
Attn: Dr. R.L. Park
College Park, MD 20742

University of Minnesota
Electrical Engineering Dept
Attn: Dr. W.T. Peria
Minneapolis, MN 55455

City University of New York
Attn: Dr. N. Tzoar
Convent Ave at 138th St
New York, NY 10031

Univ of California at Irvine
Department of Physics
Attn: R.F. Wallis
Irvine, CA 92664

Northwestern University
Dept of Physics
Attn: Dr. Chia-Wei Woo
Evanston, IL 60201

James Franck Institute
Dept of Chemistry
Attn: Dr. Lennard Wharton
5640 Ellis Ave
Chicago, IL 60637

MIT
Department of Chemistry Room6335
Attn: Dr. M.S. Wrighton
Cambridge, MA 02139

University of Wisconsin
Dept of Metallurgical & Mining
Engineering
Attn: Dr. M.G. Lagally
Madison, WI 53706

Yeshiva University
Physics Dept
Attn: Dr. D.C. Mattis
Amsterdam Ave & 185th St
New York, NY 10033

James Franck Institute
Department of Chemistry
Attn: Dr. R. Gomer
5640 Ellis Ave
Chicago, IL 60637

Director, Defense Adv Res Proj
Attn: Technical Library
1400 Wilson Blvd
Arlington, VA 22209
(3)

Office of Naval Research
Physics Program Office (Code 421)
800 North Quincy Street
Arlington, VA 22217
(3)

Office of Naval Research
Asst Chief for Tech (Code 200)
800 North Quincy Street
Arlington, VA 22217

Office of Naval Research
Chemistry Program (Code 472)
800 North Quincy Street
Arlington, VA 22217

Naval Research Laboratory
Attn: Technical Library
Washington, DC 20375
(3)

Office of Director of Defense
Research & Engineering
Info Office Library Branch
The Pentagon
Washington, DC 20375 (3)

U.S. Army Research Office
Box CM, Duke Station
Durham, NC 27706
(2)

Defense Documentation Center
Cameron Station
Alexandria, VA 22314
(12)

Director, National Bureau of
Standards
Attn: Technical Library
Washington, DC 20234

Director
Office of Naval Research
Branch Office
536 South Clark St
Chicago, IL 60605
(3)

San Francisco Area Office
Office of Naval Research
One Hallidie Plaza Suite 601
San Francisco, CA 94102
(3)

Office of Naval Research
Code 102 IP (ONRL)
800 North Quincy Street
Arlington, VA 22217
(6)

Air Force Office of Scientific
Research
Department of the Air Force
Washington, DC 22209

Director
Office of Naval Research
Branch Office
1030 East Green Street
Pasadena, CA 91101
(3)

Director
Office of Naval Research
Branch Office
495 Summer Street
Boston, MA 02210
(3)

Director, U.S. Army Eng Res
& Development Labs
Attn: Tech Documents Center
Fort Belvoir, VA 22060

ODDR&E Advisory Group on
Electron Devices
201 Varick Street
New York, NY 10014
(3)

New York Area Office
Office of Naval Research
715 Broadway, 5th Floor
New York, NY 10003

Air Force Weapons Laboratory
Technical Library
Kirtland AFB
Albuquerque, NM 87118

Air Force Avionics Laboratory
Air Force Systems Command
Technical Library
Wright-Patterson AFB, OH 45433

Air Force Cambridge Res Lab
L.G. Hanscom Field
Technical Library
Cambridge, MA 01238

Harry Diamond Labs
Technical Library
Connecticut Ave at Van Ness NW
Washington, DC 20008

Naval Air Development Center
Attn: Technical Library
Johnsville
Warminster, PA 18974

Naval Weapons Center
Technical Library (Code 753)
China Lake, CA 93555

Naval Training Equipment Ctr
Technical Library
Orlando, FL 32813

Navy Underwater Systems Center
Technical Library
New London, CN 06320

Commandant of the Marine Corps
Scientific Advisor (Code RD-1)
Washington, DC 20380

Naval Ordnance Station
Technical Library
Indian Head, MD 20640

Naval Postgraduate School
Technical Library (Code 0212)
Monterey, CA 93940

Naval Missile Center
Technical Library (5632.2)
Point Mugu, CA 93010

Naval Ordnance Station
Technical Library
Louisville, KY 40214

Naval Oceanographic Office
Tech Library (Code 1600)
Washington, DC 20373

Naval Explosive Ordnance
Disposal Facility
Technical Library
Indian Head, MD 20640